

# Synthesis and processing of CdS/ZnS multilayer films for solar cell application

Isaiah O. Oladeji, Lee Chow\*

*Department of Physics, University of Central Florida, Orlando, FL 32816-2385, USA*

Received 29 July 2003; received in revised form 11 August 2004; accepted 11 August 2004

Available online 12 October 2004

## Abstract

We demonstrate that homogeneous  $\text{Cd}_{1-x}\text{Zn}_x\text{S}$  thin films can be synthesized from chemical bath deposited CdS/ZnS multilayers through low-temperature chemical and thermal-activated diffusion. The secondary ion mass spectrometry depth profiles indicate that Cd diffuses into ZnS film more readily than Zn diffuses into CdS film. We also demonstrated how this approach could be used in improving the spectral response of CdTe-based solar cells.

© 2004 Elsevier B.V. All rights reserved.

*Keywords:* Chemical bath deposition; CdS thin films; ZnS thin films; Solar cell

## 1. Introduction

The zinc-based binary and ternary II–VI compounds (ZnS,  $\text{Cd}_{1-x}\text{Zn}_x\text{S}$ , ZnSe, and  $\text{Cd}_{1-x}\text{Zn}_x\text{Se}$ ) are of great importance in the optoelectronic application [1,2]. Because of their bandgaps, any of these materials, could be an excellent window layer in CdTe thin film solar cells. Since chemical bath deposition (CBD) is known to produce solar cell grade films over a large area at a low cost and low temperature, efforts have been made by many researchers [3–10] over the years to grow these materials by this method. However, because of difficulties in growing the films of these chalcogenides of zinc by CBD in the basic aqueous medium there seem to be some controversies in the reported results.

For example, Chu [3] used  $\text{NH}_3$  as the complexing agent in the synthesis of  $\text{Cd}_{1-x}\text{Zn}_x\text{S}$  films with no success. Whereas Sharma and Garg [4], with the same  $\text{NH}_3$  as a ligand grew  $\text{Cd}_{1-x}\text{Zn}_x\text{Se}$  (with  $0 \leq x \leq 1$ ) films. Padam and Malhotra [5] with triethanolamine (TEA) and  $\text{NH}_3$  as ligands reported the growth of  $\text{Cd}_{1-x}\text{Zn}_x\text{S}$  throughout the

composition range ( $0 \leq x \leq 1$ ). However, Pramanik and Biswas [6], also using TEA and  $\text{NH}_3$  as complexing agents for the growth of ZnSe films, reported that film or precipitate formation is impossible without hydrazine ( $\text{N}_2\text{H}_4$ ) presence in the reaction bath. Dona and Herrero [7], with  $\text{NH}_3$  as the major and  $\text{N}_2\text{H}_4$  as the complementary complexing agents, reported the growth of ZnS films. The latter went further to say that the presence of  $\text{N}_2\text{H}_4$  is not essential, but its absence causes a very low grow rate (about  $5 \text{ \AA}/\text{min}$ ); and its presence improves the homogeneity and specularity of the film. Estrada et al. [8], on the other hand, used  $\text{NH}_3$  and citrate ions as complexing agents in the growth of ZnSe and recorded a success. Yamaguchi et al. [9] also reported a CBD of (Cd, Zn)S films with  $\text{NH}_3$  and  $\text{I}^-$  as complexing agent, when the reagents are mixed together in certain order. Recently, Oladeji and Chow [10] performed a battery of experiments using  $\text{NH}_3$  and  $\text{N}_2\text{H}_4$  as complexing agents separately and together in the growth of ZnS thin films. When these agents are used separately they reported that negligible film growth takes place. However, they succeeded in growing films when both agents are used together.

We first note that the hydrolysis of thiourea and selenourea, the precursors of S and Se, respectively, are similar in a basic aqueous bath. Thus, the ability to grow the

\* Corresponding author. Tel.: +1 407 823 2325; fax: +1 407 823 5112.

E-mail address: [chow@ucf.edu](mailto:chow@ucf.edu) (L. Chow).

Zn-based materials of these chalcogens by CBD depends on Zn or any other constituent metal. Now, from the revelation above, it is apparent that for the growth of ZnS or ZnSe films by CBD in a basic aqueous bath, if  $\text{NH}_3$  is used as a complexing agent, there is a need for either  $\text{N}_2\text{H}_4$  or citrate ion or iodine ion as the secondary complexing agent. In our previous work [10] based on the analytical and experimental studies of the CBD growth mechanisms of ZnS thin film in a hydrazine–ammonia medium, we rationalize our observation by the following arguments:

- (1) In the  $\text{NH}_3$  only medium, the Zn–amine complex is mostly in the form  $[\text{Zn}(\text{NH}_3)_4]^{2+}$  with  $10^{8.9}$  [7] as the stability constant ( $k$ ). This high  $k$  value in our opinion prevents the complex ion from being easily adsorbed by the substrate, or if absorbed the zinc–ligand bonds of the complex do not relax for the heterogeneous reaction with S precursor to take place; and no film grows.
- (2) On the other hand, in the bath containing  $\text{N}_2\text{H}_4$  as the only complexing agent, the Zn complex is predominantly in the form  $[\text{Zn}(\text{N}_2\text{H}_4)_3]^{2+}$  with  $k=10^{5.5}$  [7,11]. This low  $k$  value encourages Zn ion presence in a concentration which, together with S ion, allows a homogeneous reaction instead of a heterogeneous reaction necessary for the film growth to take place; and no film grows either.
- (3) From our experience, CdS and CdSe thin films are easily grown by CBD with  $\text{NH}_3$  as the complexing agent. Thus,  $[\text{Cd}(\text{NH}_3)_4]^{2+}$  being the major precursor in the heterogeneous growth of CdS and CdSe thin films [12] with  $k=10^{6.9}$ , it is logical to infer that a metallic complex that can partake in CBD must have a stability constant that is about this value. That we are able to grow ZnS film when  $\text{NH}_3$  and  $\text{N}_2\text{H}_4$  are present together in the same bath indicates that Zn complex that satisfies the latter condition is present. This is found to be true if  $\text{N}_2\text{H}_4$  concentration is about twice [6] that of  $\text{NH}_3$ . Since the Zn– $\text{NH}_3$  complex has a higher  $k$  than the Zn– $\text{N}_2\text{H}_4$  complex, we can infer that the common ion effect, or some other effects not known to us, forced most of the Zn– $\text{NH}_3$  complex to acquire the form  $[\text{Zn}(\text{NH}_3)_3]^{2+}$ . The stability constant of the latter [11] is  $10^{6.6}$ . This value is moderate and a lot closer to the magical  $10^{6.9}$  number quoted above, and makes this complex conform to CBD growth mechanism, in other words, it makes  $[\text{Zn}(\text{NH}_3)_3]^{2+}$  a major Zn precursor in the ZnS film growth. Similar arguments can equally be applied for  $\text{NH}_3$ –citrate ion bath and  $\text{NH}_3$ – $\text{I}^-$  ion bath. O'Brien et al. [13] and Bayer et al. [14] in their recent articles have supported this view and the argument advanced here.

Now, for the growth of  $\text{Cd}_{1-x}\text{Zn}_x\text{S}$  or  $\text{Cd}_{1-x}\text{Zn}_x\text{Se}$ , the reaction bath must contain  $\text{N}_2\text{H}_4$  (our preferred choice) for the Zn element to be incorporated in the film. Unfortunately,

the chemical effect of  $\text{N}_2\text{H}_4$  on the Zn–amine complex is similar to that of the Cd–amine complex. This means more Cd–amine complex will exist in the form  $[\text{Cd}(\text{NH}_3)_3]^{2+}$ . Since the unsaturated Cd–amine complex,  $[\text{Cd}(\text{NH}_3)_3]^{2+}$  with [11]  $k=10^{6.2}$  is less stable than that of Zn, the concentration of  $\text{Cd}^{2+}$  present in the bath is high and together with  $\text{S}^{2-}$  or  $\text{Se}^{2-}$  concentration they easily exceed the solubility product constant of CdS or CdSe. Homogeneous reaction resulting into CdS or CdSe colloid formation therefore dominates the reaction. These colloids eventually induce  $\text{Cd}_{1-x}\text{Zn}_x\text{S}$  or  $\text{Cd}_{1-x}\text{Zn}_x\text{Se}$  precipitation. Extensive work on the growth of  $\text{Cd}_{1-x}\text{Zn}_x\text{S}$  films during the course of this study in the hydrazine–ammonia medium always leads to negligible film growth and mostly the precipitation of ternary compounds, confirming the argument above. An alternative way of synthesizing the  $\text{Cd}_{1-x}\text{Zn}_x\text{S}$  thin films by CBD for solar cell application was therefore sought.

This study focuses on (1) improving the quality of CBD grown ZnS thin films, (2) synthesizing ZnS/CdS multilayer films and finding how chemical and thermal activated interdiffusion between these layers can be used to convert this multilayer to  $\text{Cd}_{1-x}\text{Zn}_x\text{S}$  films for optoelectronic applications.

## 2. Experimental details

From our previous work [10], it is observed that the growth of ZnS thin film at room temperature in  $\text{NH}_3/\text{N}_2\text{H}_4$  medium leads to less adherent thicker film. Although the growth at temperatures higher than the room temperature improves somewhat the adherence, the excessive homogeneous reaction that comes with this approach minimizes the heterogeneous reaction, hence the resulting minimum film thickness. As a result, for the growth of adherent thicker ZnS thin films at about  $55^\circ\text{C}$ , potassium nitrilotriacetate (KNTA) was introduced as an additional complexing agent.

The experimental procedure for growing ZnS thin films is the same as described previously [10], with the exception that KNTA was added to the reaction bath after  $\text{NH}_4\text{OH}$  and prior to adding  $\text{N}_2\text{H}_4 \cdot \text{H}_2\text{O}$ . The growth of CdS layers, on the other hand, followed the same procedure as described in Ref. [15]. With the CBD growth of ZnS and CdS already well established, we dipped the substrate into ZnS and CdS growth bath one after the other to grow ZnS/CdS multilayer structures. The substrates used in this experiment are either quartz glass or transparent conducting oxide coated soda lime glass (TCO/glass).

The grown films were annealed in argon ambient at  $400^\circ\text{C}$ . The CdS, ZnS, and CdS/ZnS multilayer films were annealed for 60 min. Ultraviolet–visible (UV–VIS) spectrophotometer, secondary ion mass spectrometry (SIMS), Rutherford backscattering (RBS), and X-ray diffraction (XRD) were used to characterize both annealed as well as unannealed films. Film thickness was measured by an Alpha-step profilometer.

The SIMS data were taken using a CAMECA IMS-3f with  $O_2^+$  primary beam and detection of secondary positive ions. The impact energy was 5.5 keV. Typical sputtering conditions were 150 nA  $O_2^+$  into  $200 \times 200 \mu\text{m}$  crater. Ions were detected from a  $60\text{-}\mu\text{m}$  diameter region at the center of the crater.

For the RBS, 2.25 MeV  $\alpha$ -particles were used as incident ions. The detection of backscattered particles was at  $164.2^\circ$  relative to the incident beam and the energy resolution of the system was 13 keV.

### 3. Results and discussions

#### 3.1. ZnS thin film grown from $NH_3/N_2H_4$ aqueous medium

Fig. 1 shows the RBS spectrum of ZnS film grown on quartz glass from  $NH_3/N_2H_4$  medium. Apart from the Si and O signals from the substrate, there are Zn and S peaks emanating from the film. The thickness of the ZnS film after three dips is about 100 nm; and we cannot tell whether there is any contribution to the oxygen signal in the spectrum from the film. These films absorb water vapor and become powdery within a few days after growth. A freshly grown film also has poor adherence to the substrate. All these characteristics do not make these ZnS films suitable for any applications.

#### 3.2. ZnS thin film grown from $NH_3/N_2H_4/KNTA$ aqueous medium

To improve the quality of ZnS films, KNTA was introduced in the reaction bath as an additional complexing agent. The optimum concentration of KNTA is found to be 0.5 g in 140-ml solution. The ZnS thin film grown from this reaction bath has a saturation thickness that is about 1200 Å as against 350 Å reported for  $NH_3/N_2H_4$  only containing

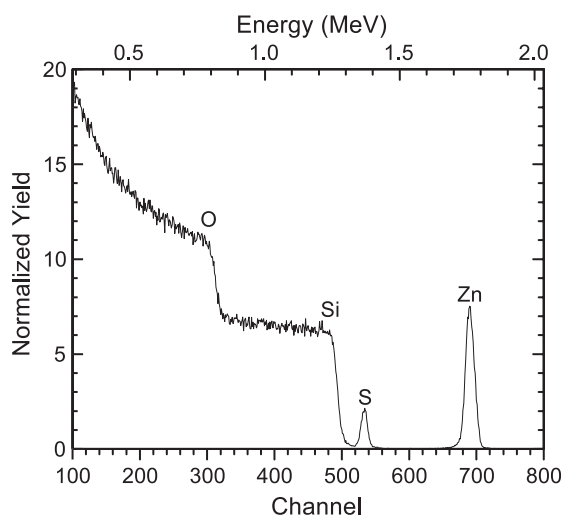


Fig. 1. RBS spectrum of ZnS thin film deposited from  $NH_3/N_2H_4$  aqueous medium on a quartz glass. The film thickness is about 0.10  $\mu\text{m}$ .

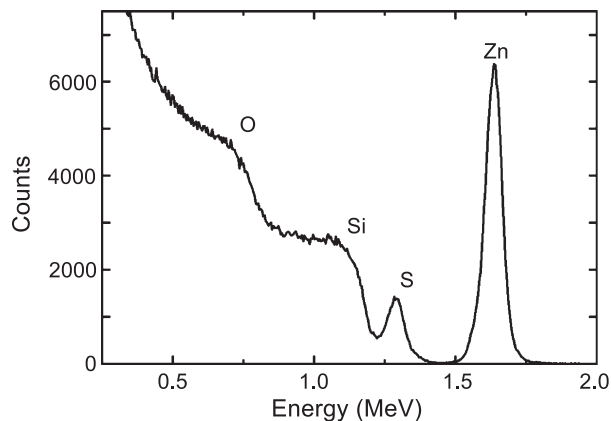


Fig. 2. RBS spectrum of ZnS thin film deposited from  $NH_3/N_2H_4/KNTA$  aqueous medium on a quartz glass. The film thickness is about 0.15  $\mu\text{m}$ .

bath above room temperature [10]. The films are specularly reflecting and colorless. The adherence of the film to the substrate is much better than that grown from  $NH_3/N_2H_4$ -only media. Also, the films do not deteriorate in quality with time.

Fig. 2 shows the RBS spectrum of ZnS thin film deposited on quartz glass from  $NH_3/N_2H_4/KNTA$  aqueous bath. In this bath, the addition of KNTA seems to have a major effect on the ZnS film growth. It increases the growth rate and also improves the quality of the ZnS films. The analysis of the spectrum revealed [16] that the film is stoichiometric with a Zn-to-S ratio of 1.02, a behavior that is native to CBD grown films from a stable bath.

The XRD study of the films did not reveal any well-defined peaks, indicating a highly disordered material, similar to that previously reported by Dona and Herero [7]. Fig. 3 shows the XRD pattern of ZnS precipitate collected from the reaction bath. The  $2\theta$  peaks at  $28.25^\circ$ ,  $47.9^\circ$ , and  $56.75^\circ$  correspond [17] to reflections from (002), (110), and (201) planes of wurtzite-2H ZnS phase, respectively. These peaks are quite broad, which is indicative [18] of nanosize particle. Generally, in chemical bath deposition, the average particle size of the precipitate is usually much larger than the average grain size of the

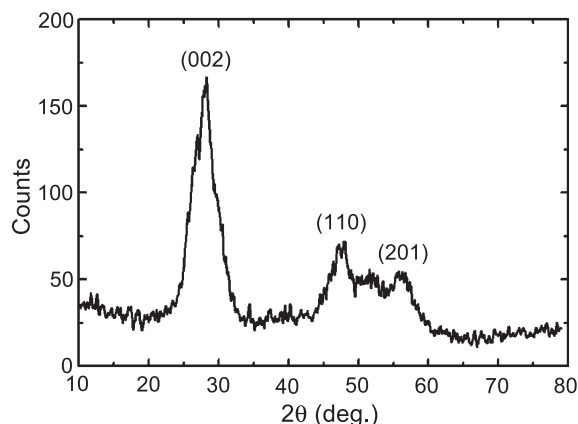


Fig. 3. XRD pattern of ZnS precipitate collected from the reaction bath.

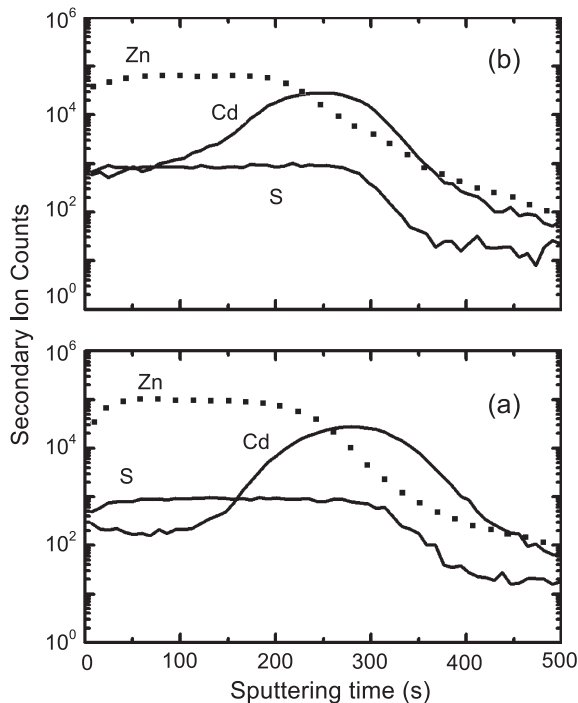


Fig. 4. SIMS depth profile of (a) unannealed and (b) annealed CBD-grown ZnS/CdS bilayer film structures on TCO/glass.

polycrystalline film [19]. Thus, the precipitate particle size being in the nanometer range, it makes sense to believe that the grown film is amorphous; this explains why the X-ray results of CBD grown ZnS films are featureless.

### 3.3. CdS/ZnS multilayer

Fig. 4(a) and (b) shows the SIMS depth profile of CdS/ZnS bilayer before and after annealing on TCO/glass substrate. We observe in these figures that S secondary ion count is relatively constant throughout the structure. Since there is no change in the S ion count to differentiate between the ZnS and CdS layers, we can infer that the mechanisms of growth of these two materials are similar. Moreover, RBS has revealed that the ratio of Cd to S and Zn to S in CBD grown CdS [20] and ZnS films are 1.00 and 1.02, respectively. Therefore, extrapolating the growth behavior of CBD-ZnS film from the already established CBD-CdS film as we have done here is reasonable.

In the SIMS analysis using Cd as a reference, points at which the count is 50% of the peak Cd count mark the approximate position of the CdS layer edges. At the leftmost edge of the CdS layer, located between 200 and 250 s, in Fig. 4(a), the Zn ion count is just slightly lower than its peak count. This observation implies that some intermixing between the two layers has taken place prior to annealing, perhaps due to chemical activated ion exchange diffusion into the CdS on TCO/glass substrate during ZnS growth. Fig. 4(b) shows the SIMS depth profile of the same ZnS/CdS bilayer after annealing. In this figure, the Cd secondary ion count at the center of ZnS layer has increased by about

400%, whereas that of Zn at the center of CdS layer has increased by only 50% of their counts as grown. These clearly indicate that we have more Cd diffusing into ZnS than Zn diffusing into CdS; a phenomenon that may be of great interest in the realization of the new solar cell window layer in the future.

For further studies on the interdiffusion between layers, we consider Fig. 5(a) and (b) which shows the SIMS depth profile of several layers of CdS and ZnS stacked on top of each other in the form ZnS/CdS/ZnS/CdS/TCO/glass structure. In the unannealed sample, Fig. 5(a), the Cd secondary ion count at the center of the ZnS layer sandwich between the two adjacent CdS layers is about 80% of its peak count. And it appears that intermixing of ZnS and CdS has taken place throughout this ZnS layer. However, if we look at the last three layers where CdS is sandwiched between two ZnS layers, we see that the ZnS layers are still very distinct. In fact, the Zn secondary ion count at the center of CdS layer is about 5% of its average peak count. Based on these observations, one can say that chemically activated diffusion of Cd into ZnS film takes place more readily when a ZnS-coated substrate is dipped into CdS growth bath than Zn will do into CdS film when it is dipped into ZnS growth bath.

Fig. 5(b) shows the SIMS depth profile of the same sample in Fig. 5(a) after 400 °C thermal annealing. Here, at the center of the last ZnS layer, the Cd ion count has increased by about 4200% of its count prior to annealing. The thermal activated diffusion seems to have increased the overall mixing of the layers. This latter has resulted in about 30% fluctuation of the Cd count about its average count

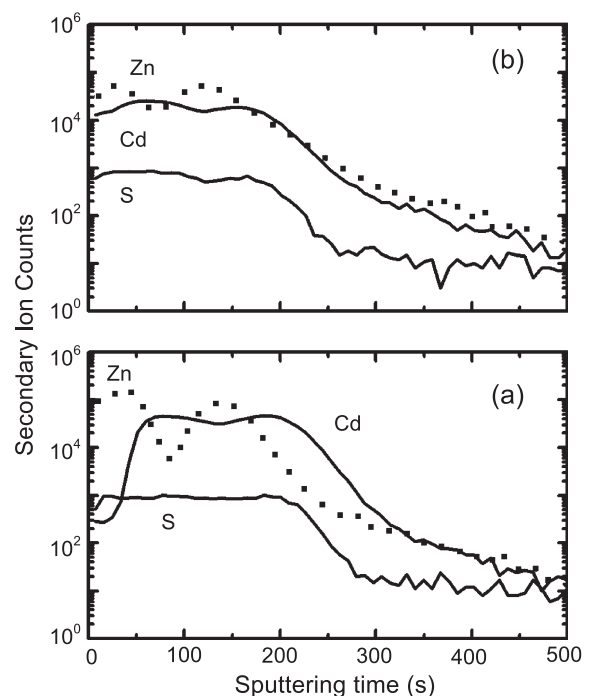


Fig. 5. SIMS depth profile of (a) unannealed and (b) annealed CBD-grown ZnS/CdS/ZnS/CdS multilayer film structures on TCO/glass.

throughout the structure while that of Zn is about 60%. All these observations have allowed us to infer that Cd may be more mobile in this structure than Zn not only during thermal activated diffusion but also during chemical activated diffusion. The diffusion coefficient of Cd, which is also a measure of mobility, was previously reported [21] to increase with increase in  $x$  or Cd content in  $\text{Zn}_{1-x}\text{Cd}_x\text{S}$  and this confirms our observation about the highly mobile Cd. It is also obvious from Figs. 4 and 5 that stacked thin layers of CdS and ZnS respond faster to intermixing processes than stacked thick layers as expected.

The plot of absorption coefficient squared ( $\alpha^2$ ) versus photon energy ( $h\nu$ ) of various types of ZnS/CdS structures on quartz glass compare to pure CdS and ZnS thin films also on quartz glass prior to annealing and after annealing are shown in Figs. 6 and 7, respectively. We observe that the absorption edges of the films especially CdS (Fig. 7a) and ZnS (Fig. 7e) films have red-shifted after annealing, perhaps due to an increase in grain sizes of the polycrystalline film.

Fig. 6(d) shows that the unannealed bilayer structure has a broad absorption edge of  $\text{Cd}_{1-x}\text{Zn}_x\text{S}$  with a continuously changing  $x$  value. However, in Fig. 7(d), the  $\alpha^2$  versus the  $h\nu$  plot of the annealed bilayer shows almost two distinct band edges corresponding to a region of high fixed Zn content and a region of low fixed Zn content. The region of high Zn content seems to be much thicker than the other region. This means that thermal annealing has almost homogenized the ZnS/CdS bilayer. This homogenization is made possible mostly by Cd diffusion, since the Cd-rich layer has almost disappeared as depicted by Fig. 7(d). This observation further supports the fact that more Cd diffuses into ZnS layer than the other way around.

Figs. 6(b) and 7(b) are the  $\alpha^2$  versus  $h\nu$  plots of unannealed and annealed CdS/ZnS/CdS structures, respectively. The absorption edge of this structure in both cases appears sharp and located in the slightly higher energy portion of the spectrum compared to CdS absorption edge (Figs. 6a and 7a). The sharp absorption is characteristic of

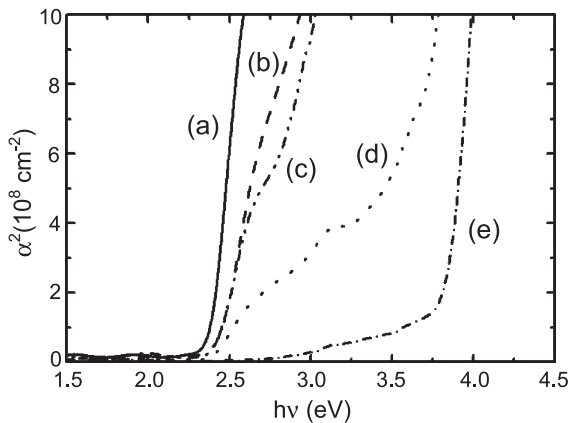


Fig. 6.  $\alpha^2$  versus  $h\nu$  plot of unannealed CBD-grown ZnS/CdS structures on quartz glass. (a) CdS, (b) CdS/ZnS/CdS, (c) ZnS/CdS/ZnS/CdS, (d) ZnS/CdS, (e) ZnS.

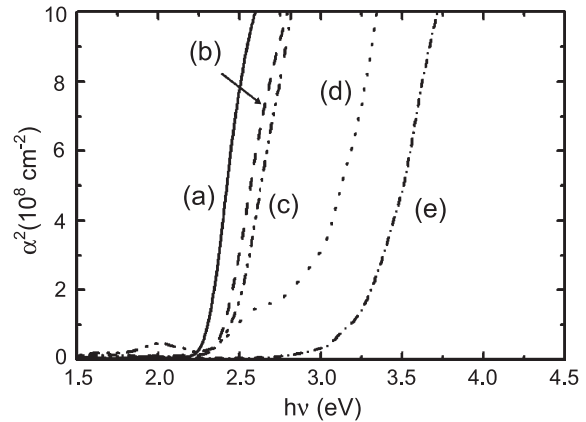


Fig. 7.  $\alpha^2$  versus  $h\nu$  plot of annealed CBD-grown ZnS/CdS structures on quartz glass. (a) CdS, (b) CdS/ZnS/CdS, (c) ZnS/CdS/ZnS/CdS, (d) ZnS/CdS, (e) ZnS.

a homogeneous structure, in other words  $\text{Cd}_{1-x}\text{Zn}_x\text{S}$  with a fixed  $x$  value. This observation is in agreement with the portion of Fig. 5 that profiles the ZnS layer sandwiched between two CdS layers. In this structure, the intermixing of ZnS and CdS is almost complete prior to annealing owing to chemical activated diffusion. The implication of all these is that a homogeneous  $\text{Cd}_{1-x}\text{Zn}_x\text{S}$  can be fabricated from the CdS/ZnS/CdS structure at a temperature less than 100 °C.

Figs. 6(c) and 7(c) depicted  $\alpha^2$  versus  $h\nu$  plot of the ZnS/CdS/ZnS/CdS structure before and after annealing, respectively. The plot of the unannealed structure (Fig. 6c), shows two adsorption edges: a sharp one that is indicative of  $\text{Cd}_{1-x}\text{Zn}_x\text{S}$  with a low fixed  $x$  value, and the broad absorption edge corresponding to  $\text{Cd}_{1-x}\text{Zn}_x\text{S}$  with graded higher  $x$  values. These observations agree with the SIMS depth profile (Fig. 5a), of this same structure. The  $\alpha^2$  versus  $h\nu$  plot of the annealed structure (Fig. 7c), shows a single sharp absorption edge in the energy region lying between the absorption edges of ZnS (Fig. 7e), and CdS (Fig. 7a).

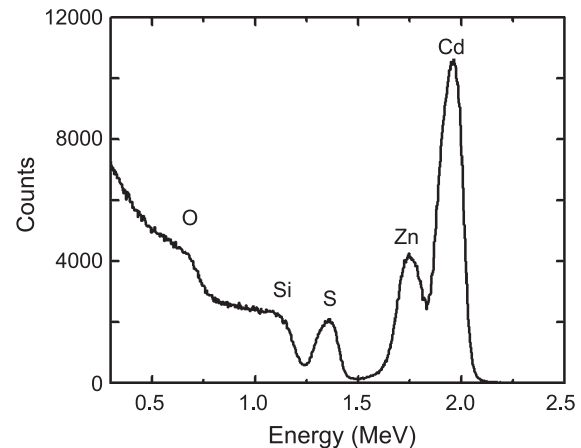


Fig. 8. RBS spectrum of annealed ZnS/CdS/ZnS/CdS structure on quartz glass.

This absorption edge is clearly that of the homogeneous  $\text{Cd}_{1-x}\text{Zn}_x\text{S}$  film. The SIMS depth profile of this same structure (Fig. 5b), depicts it to be somewhat homogeneous. A further test of homogeneity was carried out by RBS. The RBS spectrum (Fig. 8) shows that the annealed structure is homogeneous, for the width of Cd, Zn, S peaks are nearly equal. The estimated composition [16] is  $\text{Cd}_{0.55}\text{Zn}_{0.45}\text{S}$ . Hence, chemical and thermal activated diffusion can be used to achieve homogeneous  $\text{Cd}_{1-x}\text{Zn}_x\text{S}$  thin film from the CBD grown stacked ZnS and CdS thin films.

### 3.4. Applications

In the solar cell of CdTe, the lattice mismatch between n-CdS and p-CdTe and the low bandgap of CdS window layer are known [22,23] to have some drawback on cell performance. Using higher bandgap materials [23] like ZnS or  $\text{Cd}_{1-x}\text{Zn}_x\text{S}$  as a heterojunction partner to CdTe can improve the window bandgap, but the lattice mismatch of these materials is worse than that of CdS. Trading off the latter mismatch for the higher bandgap may not be the solution, for the loss in cell performance [23] due to lattice mismatch outweighs the gain due to the increase in window bandgap. Therefore, to retain the compatibility of CdS and CdTe and still improve the short wavelength spectral response of CdTe solar cell, its traditional CdS/CdTe structure should be changed to  $\text{Cd}_{1-x}\text{Zn}_x\text{S}/\text{CdS}/\text{CdTe}$ . In other words, a  $\text{Cd}_{1-x}\text{Zn}_x\text{S}/\text{CdS}$  layer should replace the CdS-only window layer. Since the CBD-grown CdS layer has produced some of the best performing cells, the growth of the new  $\text{Cd}_{1-x}\text{Zn}_x\text{S}/\text{CdS}$  window layer by CBD should therefore be explored. To achieve the new  $\text{Cd}_{1-x}\text{Zn}_x\text{S}/\text{CdS}$  structure proposed for the CdTe window layer, what is required is simply an additional growth of CdS on top of the  $\text{Cd}_{1-x}\text{Zn}_x\text{S}$  layer obtained from a processed CBD-grown ZnS/CdS multilayer. We have reported the results of the solar cells based on this new window elsewhere [24].

For clarity, we include the performance of the proposed windows here. Three structures were fabricated on Libbey Owens Ford TEC 8 TCO coated soda lime glass of 3 mm thickness. The structures are “glass/TCO/CdS/CdTe/contact,” type 1 “glass/TCO/ $\text{Cd}_{1-x}\text{Zn}_x\text{S}/\text{CdS}/\text{CdTe}/\text{contact}$ ,” and type 2 “glass/TCO/ $\text{Cd}_{1-x}\text{Zn}_x\text{S}/\text{CdS}/\text{CdTe}/\text{contact}$ .”

In type 1 “ $\text{Cd}_{1-x}\text{Zn}_x\text{S}/\text{CdS}$ ” window, a 0.07- $\mu\text{m}$ -thick ZnS film was first deposited on TCO/glass substrate. This was then dipped in 1%  $\text{CdCl}_2$  methanol solution for about 30 s to improve the conductivity, then dried with an infrared lamp, and then rinsed in the deionized water. This was followed by an additional deposition of 0.05- $\mu\text{m}$  CdS thin film to complete the window fabrication.

In type 2 “ $\text{Cd}_{1-x}\text{Zn}_x\text{S}/\text{CdS}$ ” window, a 0.03- $\mu\text{m}$  thick CdS film, sandwiched between two 0.04- $\mu\text{m}$ -thick ZnS films, was first deposited by CBD on TCO/glass substrate. The glass multilayers substrate was then given the usual  $\text{CdCl}_2$  treatment described above. The sample was then annealed in  $\text{CdCl}_2/\text{Ar}$  ambient at 400 °C for 15 min. The

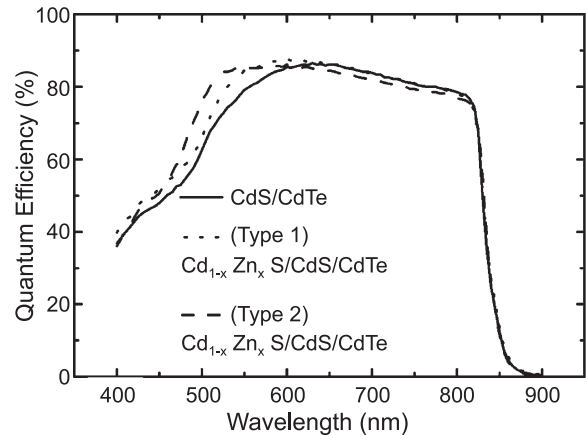


Fig. 9. Spectral response of “glass/TCO/CdS/CdTe/contact,” type 1 “glass/TCO/ $\text{Cd}_{1-x}\text{Zn}_x\text{S}/\text{CdS}/\text{CdTe}/\text{contact}$ ,” and type 2 “glass/TCO/ $\text{Cd}_{1-x}\text{Zn}_x\text{S}/\text{CdS}/\text{CdTe}/\text{contact}$ ” structures.

window fabrication was completed by the deposition of an additional 0.035- $\mu\text{m}$ -thick CdS film.

Depositing CdTe and the contact completed the structure in each case. The spectral responses of these structures are shown in Fig. 9. In the following order, CdS/CdTe, type 1, and type 2  $\text{Cd}_{1-x}\text{Zn}_x\text{S}/\text{CdS}/\text{CdTe}$  structures have 80% or slightly higher quantum efficiency (QE) in the 600–850, 525–850, and 510–850 nm wavelength regions. Below these regions, at 500 nm, say, the QE is about 62% for CdS/CdTe structure, 65% for type 1 structure, and 75% for type 2 structure; and at 400 nm, the QE are 38%, 40%, and 38% in that same order. We note that the structure with the  $\text{Cd}_{1-x}\text{Zn}_x\text{S}$  layer (type 1 and type 2 structures) generally has better short wavelength response, as expected. Thus, changing the window layer of the CdTe solar cell from CdS only to  $\text{Cd}_{1-x}\text{Zn}_x\text{S}/\text{CdS}$  may be a way of increasing the efficiency of this cell that has stagnated at 16% for more than a decade now.

## 4. Conclusions

We have demonstrated using chemical and thermal activated diffusion that  $\text{Cd}_{1-x}\text{Zn}_x\text{S}$  thin films can be synthesized from chemical bath deposited ZnS/CdS multilayers. A more homogeneous  $\text{Cd}_{1-x}\text{Zn}_x\text{S}$  film is obtained at low processing temperature if the stacked layers are thin. Of great importance is that the grown structure is almost homogenized in the chemical bath at the temperature below 100 °C. The SIMS depth profile of our structure reveals that the low temperature chemical activated ion exchange diffusion of Cd into ZnS film takes place more readily if ZnS coated substrate is dipped in CdS growth bath. On the other hand, the diffusion of Zn into CdS film dipped in ZnS growth bath occurs only slowly. Nevertheless, the homogenization of our structure is achieved by annealing at 400 °C, the temperature generally used for processing solar cells. The low

processing temperature developed here in the fabrication of  $\text{Cd}_{1-x}\text{Zn}_x\text{S}$  means that the proposed  $\text{Cd}_{1-x}\text{Zn}_x\text{S}/\text{CdS}$  solar cell window could be grown at temperatures that will not damage the glass or the underlying transparent conducting oxide generally used as substrate in solar cells. This method, since it is based on chemical bath deposition and a thermal process that does not exceed  $400\text{ }^\circ\text{C}$ , has the potential of greatly impacting the solar cell industries.

### Acknowledgement

We would like to thank Mr. Fred Stevie of North Carolina State University for the SIMS measurements, Dr. Gabriel Braunstein of UCF for the RBS measurements, and Dr. A. N. P. Bustamante of Center for Research and Education in Optics and Lasers for the XRD measurements. We also appreciate very much Dr. C. S. Ferekides of the University of South Florida for growing the CdTe film. Technical support from the staff of Agere/UCF Material Characterization Facility (MCF) is greatly appreciated.

### References

- [1] S. Ignatowicz, A. Kobendza, *Semiconductor Thin Films of A<sup>II</sup>B<sup>VI</sup> Compounds*, John Wiley & Sons, New York, 1990.
- [2] H. Mar, in: H.E. Ruda (Ed.), *Widegap II–VI Compounds for Optoelectronic Applications*, Chapman & Hall, New York, 1992, Chap. 7.
- [3] T.L. Chu, *Thin Film Cadmium Telluride, Zinc Telluride, and Mercury Zinc Telluride Solar Cells*, NREL final subcontract report, #XL-8-18091-1 (1991).
- [4] K.C. Sharma, J.C. Garg, *J. Phys. D: Appl. Phys.* 23 (1990) 1411.
- [5] G.K. Padam, G.L. Malhotra, *J. Appl. Phys.* 63 (1988) 770.
- [6] P. Pramanik, S. Biswas, *J. Electrochem. Soc.* 135 (1986) 350.
- [7] J.M. Dona, F.J. Herrero, *J. Electrochem. Soc.* 141 (1994) 205.
- [8] C.A. Estrada, P.K. Nair, M.T.S. Nair, R.A. Zingaro, E.A. Mayers, *J. Electrochem. Soc.* 141 (1994) 802.
- [9] T. Yamaguchi, Y. Yamamoto, T. Tanaka, Y. Demizu, A. Yoshida, *Thin Solid Films* 281–282 (1996) 375.
- [10] I.O. Oladeji, L. Chow, *Thin Solid Films* 339 (1999) 148.
- [11] K.B. Yatsimirskii, V.P. Vasil'Ev, *Instability Constant of Complex Compounds*, D. van Nostrand, New York, 1960, p. 105.
- [12] R. Ortega-Borges, D. Lincot, *J. Electrochem. Soc.* 140 (1993) 3464.
- [13] P. O'Brien, D.J. Otway, D. Smyth-Boyle, *Thin Solid Films* 361–361 (2000) 17.
- [14] A. Bayer, D.S. Boyle, P. O'Brien, *J. Mater. Chem.* 12 (2002) 2940.
- [15] I.O. Isaiah, L. Chow, *J. Electrochem. Soc.* 144 (1997) 2342.
- [16] W. Chu, J.W. Mayer, M.A. Nicolet, *Backscattering Spectroscopy*, Academic Press, New York, 1978.
- [17] JCPDS database, card # 36-1450.
- [18] S. Gorer, D. Hodes, *J. Phys. Chem.* 98 (1994) 5338.
- [19] D. Lincot, R. Oraga, M. Forment, *Philos. Mag.*, B 68 (1993) 185.
- [20] I.O. Isaiah, L. Chow, J.R. Liu, W.K. Chu, A.N.P. Bustamante, C. Fredricksen, A.F. Schulte, *Thin Solid Films* 359 (2000) 154.
- [21] D. Shaw, in: H.E. Ruda (Ed.), *Wide Gap II–VI Compounds for Optoelectronic Applications*, Chapman & Hall, New York, 1992, Chap. 10.
- [22] T.L. Chu, S.S. Chu, S.T. Ang, *J. Appl. Phys.* 64 (1988) 1233.
- [23] T.L. Chu, S.S. Chu, J. Britt, C. Ferekides, C.Q. Wu, *Proceedings of 22nd IEEE Photovoltaic Specialist Conference*, 1991, pp. 1136.
- [24] I.O. Oladeji, L. Chow, C.S. Ferekides, V. Viswanathan, Z. Zhao, *Sol. Energy Mater. Sol. Cells, Lett.* 61 (2000) 203.